

RecoverMark: Robust Watermarking for Localization and Recovery of Manipulated Faces

Haonan An¹ Xiaohui Ye³ Guang Hua^{2*} Yihang Tao¹ Hangcheng Cao¹
 Xiangyu Yu³ Yuguang Fang^{1*}

¹City University of Hong Kong, Hong Kong ²Singapore Institute of Technology, Singapore 828608
³South China University of Technology

(haonanan2-c, yihang.tommy)@my.cityu.edu.hk, (hangccao, my.fang)@cityu.edu.hk,
 ghua@ieee.org, eeyxh2023@mail.scut.edu.cn, yuxy@scut.edu.cn

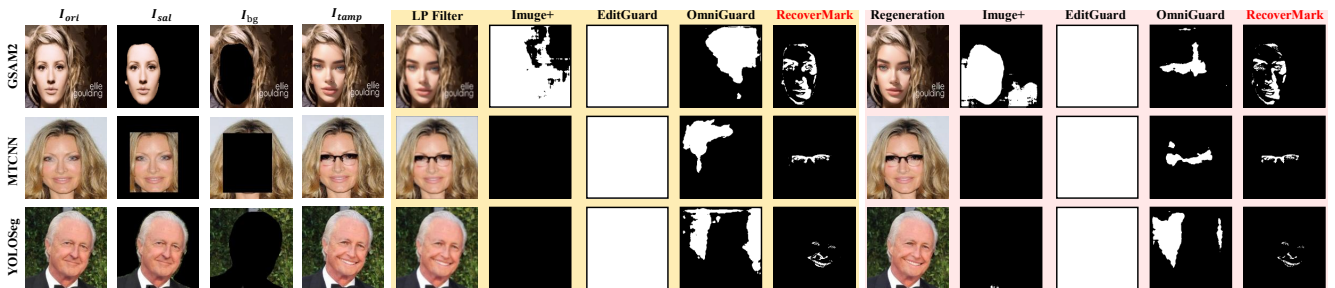


Figure 1. Visualization of face manipulation localization for Imuge+ [44], EditGuard [52], OmniGuard [53], and our proposed RecoverMark. The evaluation is conducted using three distinct region-of-interest definitions: GSAM2 [29] (face-only segmentation), MTCNN [47] (head bounding box), and YOLOSeg [37] (full-body). All methods are tested against traditional low-pass filtering and an advanced regeneration attack [54], where I_{ori} denotes the original image, I_{sal} represents segmented saliency (face), I_{bg} refers to segmented background, and I_{tamp} stands for the tampered image.

Abstract

The proliferation of AI-generated content (AIGC) has facilitated sophisticated face manipulation, severely undermining visual integrity and posing unprecedented challenges to intellectual property (IP). In response, a common proactive defense leverages fragile watermarks to detect, localize, or even recover manipulated regions. However, these methods always assume an adversary unaware of the embedded watermark, overlooking their inherent vulnerability to watermark removal attacks. Furthermore, this fragility is exacerbated in the commonly used dual-watermark strategy that adds a robust watermark for image ownership verification, where mutual interference and limited embedding capacity reduce the fragile watermark’s effectiveness. To address the gap, we propose RecoverMark, a watermarking framework that achieves robust manipulation localization, content recovery, and ownership verification simultaneously. Our key insight is twofold. First, we exploit a critical real-world constraint: an adversary must preserve the background’s semantic consistency to avoid visual detection, even if they apply global, imperceptible watermark

removal attacks. Second, using the image’s own content (face, in this paper) as the watermark enhances extraction robustness. Based on these insights, RecoverMark treats the protected face content itself as the watermark and embeds it into the surrounding background. By designing a robust two-stage training paradigm with carefully crafted distortion layers that simulate comprehensive potential attacks and a progressive training strategy, RecoverMark achieves a robust watermark embedding in no fragile manner for image manipulation localization, recovery, and image IP protection simultaneously. Extensive experiments demonstrate the proposed RecoverMark’s robustness against both seen and unseen attacks and its generalizability to in-distribution (ID) and out-of-distribution (OOD) data. Code will be released upon acceptance.

1. Introduction

Recent advances in AI-generated content (AIGC) models, such as numerous variants of Stable Diffusion [30] and GANs [8, 15], have empowered unprecedented creativity and enabled the realization of human imagination. However, these powerful techniques are double-edged swords,

*Corresponding authors.

as they can also be misused for malicious image manipulation. In particular, facial content editing has become one of the most notorious applications, raising serious concerns in morality [1], finance [34], and copyright protection [27]. Such threats not only pose a formidable challenge to media authentication but also affect the integrity of broader intelligent systems [11, 19, 35, 36].

Previous countermeasures have primarily focused on passively detecting and localizing anomalies introduced by image manipulations [12, 17, 33, 40], such as visual artifacts [16], local noise inconsistencies [24], and resolution discrepancies [20]. However, these methods often depend on prior knowledge of potential manipulation techniques, which limits their generalization to unseen or novel types of forgeries [6, 52]. To address this issue, proactive frameworks for manipulation detection and localization have been developed [3, 42, 44]. State-of-the-art methods [52, 53] in this area employ dual-watermark frameworks that combine both fragile and robust watermarks. A fragile watermark is embedded into the image before distribution and, after any manipulation, serves as a sensitive indicator to locate tampered regions. In contrast, a robust watermark, which is resistant to common image processing operations, is used concurrently for applications such as copyright authentication.

However, these methods suffer from several critical weaknesses. **1)** They rely on an implicit assumption that the image manipulator is unaware of the presence of a fragile watermark. This assumption is rather strong in practical scenarios, where an adversary can intentionally perform image post-processing operations for watermark removal attacks before or after carrying out malicious manipulations. As illustrated in Figure 1, such removal attacks (both traditional low-pass filter and advanced regeneration attack [54]) can readily corrupt the embedded fragile watermark, thereby rendering the manipulation detection and localization ineffective. **2)** In dual-watermark frameworks, the co-embedding of a robust watermark alongside the fragile one further weakens the fragile watermark’s effectiveness against removal attacks, due to mutual interference between the watermarks as well as the inherent constraints on watermark capacity. **3)** Existing methods usually neglect an equally critical aspect of watermark: the ability to recover the original content within tampered regions, which is vital for maintaining content integrity [42, 44].

To address these limitations, we propose RecoverMark, a robust watermarking framework that integrates manipulated region localization, original content recovery, and ownership verification, with a particular focus on face tampering. Our key insight is that, in practical scenarios, adversaries must preserve the background’s semantic consistency, which implies any modification should be imperceptible to human perception (this constraint does not prevent



Figure 2. A practical example when a judge determines whether the evidence is credible based on background consistency.

them from applying imperceptible post-processing to the background), to avoid being visually detected through trivial comparisons with the surrounding environment. For instance, as illustrated in Figure 2, consider an attacker attempting to evade allegations by manipulating facial regions in surveillance footage. While the face can be altered, significant background modification is infeasible, as this would introduce noticeable inconsistencies with the real environment. Such artifacts would be readily detected during judicial review, rendering the manipulated evidence unreliable. Leveraging this observation, RecoverMark segments facial content and considers it as a watermark. A two-stage, progressively trained embedding pipeline then embeds this facial watermark into the background in a robust manner, ensuring resilience against common image post-processing operations (e.g., JPEG compression, Gaussian noise, patch removal) as well as advanced removal attacks, such as the lattice attack [21] and the regeneration attack [54]. After adversarial face manipulations, RecoverMark can faithfully extract the original facial information, enabling both precise tamper localization and accurate content recovery. Moreover, since the facial watermark is embedded robustly, it also serves as a copyright verification mechanism, mitigating the vulnerabilities inherent in prior dual-watermark frameworks. Our main contributions are as follows:

- We reveal the weaknesses of the state-of-the-art proactive image manipulation localization methods and propose RecoverMark, a robust watermarking framework that simultaneously supports tamper localization, content recovery, and copyright verification, with a particular focus on face manipulation scenarios.
- We introduce a two-stage progressive training pipeline that treats facial content as a watermark and embeds it into the background in a robust manner, ensuring resilience against both common post-processing and advanced watermark removal attacks.
- We conduct extensive qualitative and quantitative experiments by using in-distribution (ID) and out-of-distribution (OOD) datasets under seen and unseen re-

removal attacks, demonstrating the generalizability, robustness, and effectiveness of RecoverMark.

2. Related Work

2.1. Passive Image Manipulation Localization

Passive methods detect inconsistencies between authentic and tampered regions using DNNs [13, 18, 40, 56]. For instance, CFL-Net [25] uses contrastive learning to maximize feature discrepancy, while MVSS-Net [6] introduces multi-view and multi-scale learning to capture robust, semantic-agnostic traces. Building upon these, MPC [23] integrates the advantages of both methods by proposing a Multi-view Pixel-wise Contrastive (MPC) algorithm. Additionally, HiFi-Net [9] and DiffForensics [45] enhance generalization by learning manipulation taxonomies and leveraging diffusion model priors, respectively. Despite these advancements, passive methods exhibit inherent limitations. Their performance degrades significantly when forensic inconsistencies in tampered regions are subtle. Furthermore, their effectiveness is often diminished in real-world applications, as crucial forensic traces can be obscured or erased by unpredictable post-processing operations during media transmission.

2.2. Proactive Image Manipulation Localization

Proactive methods share a common principle: the performance of image manipulation localization can be enhanced by embedding imperceptible redundancy into an image without significantly degrading its visual quality [32, 38, 41, 43, 55]. For instance, Asnani et al. [3] introduces a method that embeds a learned, imperceptible template into images to significantly improve the detection of manipulations and generalization against unseen AI models. Similarly, Imuge and its advanced version Imuge+ [42, 44] embed invisible noise into an image to precisely localize tampered regions. Furthermore, EditGuard [52] and its updated version OmniGuard [53] discovers that fragile watermarks, upon extraction, leave tampering artifacts at the corresponding manipulated locations. This enables precise localization of tampered areas and has achieved state-of-the-art performance in the field. However, these proactive methods are fundamentally built upon fragile watermarking, making them inherently vulnerable to watermark removal attacks, where an adversary can attempt to remove the embedded watermark before or after performing the actual manipulation.

2.3. Self-Recovery after Manipulation

Prior to the deep learning era, some methods for image manipulation address both localization and self-recovery [49–51], typically by self-embedding transformed data like DCT coefficients [10, 48]. However, these techniques are often

limited by insufficient embedding capacity. While the focus in the DNN era has shifted primarily to manipulation localization, a few recent works have revisited self-recovery. For instance, Imuge/Imuge+ [42, 44] introduces the first DNN-based framework for joint localization and recovery, and CoAtNet [26] proposes a two-level embedding mechanism only for medical images. A fundamental limitation shared by both traditional and recent self-recovery approaches is their reliance on fragile self-embedding, which makes them highly vulnerable to performance degradation from common post-processing attacks.

3. Preliminary

3.1. Tampering Localization by Fragile Watermark

To better understand the motivation behind our proposed RecoverMark, we first review the high-level workflow of prior fragile-watermark-based tampering region localization methods [52, 53] and analyze their limitations. Considering an image or a video frame I_{ori} under the threat of face manipulation, fragile-watermark-based methods first embed the fragile watermark into I_{ori} :

$$I_{\text{ctr}} = HNet(I_{\text{ori}}, I_{\text{fw}}), \quad (1)$$

where I_{ctr} is the watermarked (container) image, $HNet$ denotes the watermark hiding network, and I_{fw} is the fragile watermark image of the same size as I_{ori} . After face manipulation, the tampered I_{ctr} can be formulated as:

$$I'_{\text{ctr}} = \mathcal{N}(I_{\text{ctr}} \odot (I - M) + \mathcal{FM}(I_{\text{ctr}} \odot M)), \quad (2)$$

where I'_{ctr} is the manipulated container, \odot refers to Hadamard product, \mathcal{N} stands for the potential noise, M is the binary mask of the face region, and \mathcal{FM} represents the face manipulation operator. The embedded fragile watermark is then extracted by extraction network $ENet$:

$$I'_{\text{fw}} = ENet(I'_{\text{ctr}}). \quad (3)$$

Finally, the tampering localization mask M_{loc} is derived by comparing the extracted watermark with the original one:

$$M_{\text{loc}} = \mathbf{1}(|I'_{\text{fw}} - I_{\text{fw}}| > \text{threshold}), \quad (4)$$

where $\mathbf{1}$ is the indicator function. However, the types of \mathcal{N} considered in these methods are typically limited to traditional image post-processing operations, such as JPEG compression and Gaussian blur, while more advanced and well-studied watermark removal attacks are often overlooked. Moreover, the fragility of the embedded watermark makes it inadequate for reliable ownership verification, necessitating an additional non-fragile copyright watermark. This dual-watermark approach, however, further compromises the effectiveness of fragile watermarking due to the

inherent limited capacity for multiple watermark embeddings. Additionally, the embedded I_{fw} is independent of I_{ori} , rendering it incapable of recovering the original content after tampering.

3.2. Threat Model

We consider two adversarial parties in our threat model:

Scrutinizer. The scrutinizer has access to both the original image and the potentially manipulated version produced by the face manipulator. Before distribution, the scrutinizer proactively embeds watermarks into the original image, taking into account the risk of potential watermark removal attacks. Given a suspicious image, the scrutinizer first determines whether the facial region has been tampered with. If tampering is detected, the scrutinizer further localizes the manipulated areas of the face and restores the original content in the tampered regions.

Face Manipulator. The face manipulator has access to the watermarked image produced by the scrutinizer, seeking to alter the facial region (e.g., face swap, attribute change, and expression change) while evading detection. To do this, they may apply watermark removal attacks, ranging from common image processing to deep learning reconstruction, either before or after the manipulation.

4. Proposed Method: RecoverMark

In this section, we first present the overall workflow of RecoverMark. Next, we detail the two-stage training pipeline along with progressive training strategy. Finally, we describe how RecoverMark is applied to localize and recover tampered regions while simultaneously satisfying copyright verification requirements.

4.1. Overview

The components and the training workflow of the proposed RecoverMark are illustrated in Figure 3. The process begins by segmenting the original image I_{ori} into a saliency I_{sal} (which, in our case, corresponds to the human face content) and a background region I_{bg} , using advanced segmentation tools such as MTCNN [47], YoloSeg [37], and SAM2 [28]. Prior to watermark embedding via the hiding network $HNet$, a watermark encoder Enc compresses I_{sal} into a latent representation to better accommodate the limited watermark capacity of I_{bg} . The output of $HNet$ is the watermarked background, referred to as the container image I_{ctr} . In the first training stage, I_{ctr} is fed directly into the extraction network $ENet$ to extract the latent representation of the embedded watermark, which is further processed by watermark decoder Dec to obtain the extracted watermark I'_{sal} . In the second stage, with both the watermark encoder and decoder frozen, I_{ctr} undergoes distortion through a dedicated distortion layer, resulting in a perturbed version

I'_{ctr} , which is then input to $ENet$. The distortion layer incorporates three primary types of perturbations: saliency processing (which applies noise specifically to the salient region to discourage saliency-dependent extraction), global processing (which perturbs the entire image), and advanced attacks (such as regeneration attacks that simulate sophisticated watermark removal attacks). Together, these distortions encompass nearly all types of distortions likely to occur in real-world settings. Moreover, akin to human learning, which requires gradual acquisition of knowledge, RecoverMark also benefits from progressive exposure to distortions rather than learning them all at once. Accordingly, we introduce a progressive training strategy during the second stage, which sequentially incorporates these distortions into the training process. Further implementation details are provided in the subsequent sections.

4.2. Two-Stage Training Pipeline

4.2.1. Stage 1: Initial Training

We first segment an image or a video frame I_{ori} as:

$$I_{ori} = I_{sal} + I_{bg}, \quad (5)$$

where I_{sal} represents the salient region of interest (human face in our case), and I_{bg} corresponds to the remaining background content. Then, we formally formulate the watermark embedding process as:

$$I_{ctr} = HNet(Concat(Enc(I_{sal}), I_{bg})), \quad (6)$$

where $Concat(\cdot)$ represents channel-wise concatenation. The corresponding watermark extraction process is defined as:

$$I'_{sal} = Dec(ENet(I_{ctr})). \quad (7)$$

During the first training stage, all networks, including the watermark encoder Enc , the hiding network $HNet$, the extraction network $ENet$, and the watermark decoder Dec , are set to training mode, supervised by the following three loss functions. The first one is the fidelity loss:

$$\mathcal{L}_{Fidelity} = \sum \|I_{ctr} - I_{bg}\|_2^2, \quad (8)$$

which constrains the visual distortion introduced during watermark embedding, ensuring that the container image I_{ctr} maintains high perceptual fidelity to the original background I_{bg} . The second one is the watermark loss:

$$\mathcal{L}_{wm} = \sum \|I'_{sal} - I_{sal}\|_2^2, \quad (9)$$

which enforces the accurate extraction and decoding of the embedded saliency content. To further enhance the system's robustness and prevent false watermark detection, we introduce a clean loss defined as:

$$\mathcal{L}_{clean} = \sum \|Dec(ENet(I_{bg})) - I_{white}\|_2^2, \quad (10)$$

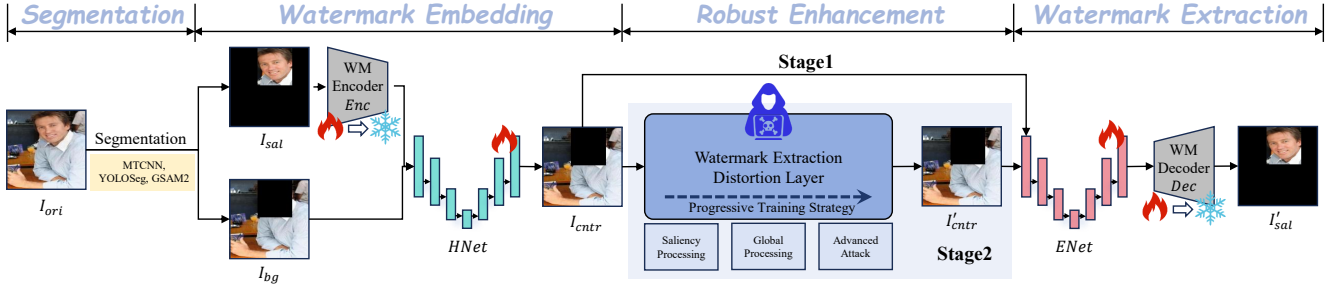


Figure 3. Flowchart of the training process for the proposed RecoverMark, where MTCNN [47] is used as segmentation model, and the watermark encoder/decoder are trained in Stage 1 but remain frozen during Stage 2.

where I_{white} is an all-white image, indicating no watermark is embedded. We jointly train these four networks by minimizing the following objective function:

$$\mathcal{L}_{\text{sum}} = \alpha_1 \mathcal{L}_{\text{fidelity}} + \alpha_2 \mathcal{L}_{\text{wm}} + \alpha_3 \mathcal{L}_{\text{clean}}, \quad (11)$$

where $\alpha_1, \alpha_2, \alpha_3$ are weighting parameters.

4.2.2. Stage 2: Robustness Enhancement Training

Stage 2 introduces a distortion layer between $HNet$ and $ENet$ to simulate adversary’s behavior and strengthen RecoverMark’s robustness against watermark removal. As Enc and Dec have already acquired stable compression and reconstruction abilities in Stage 1, they remain frozen in this phase. The watermark extraction (7) is thus updated to operate on the distorted container image I'_{ctr} :

$$I'_{\text{sal}} = Dec(ENet(I'_{\text{ctr}})). \quad (12)$$

Despite the altered input caused by distortions, the training objectives remain minimizing (11), since the distortion layer is considered an external perturbation rather than a change in the learning targets.

The design of the distortion layer is critical, as a comprehensive simulation of diverse attack types significantly enhances the general robustness of RecoverMark. However, overly complex distortions can destabilize the training process and hinder convergence. Therefore, it is essential to first classify these distortions to understand their individual properties. Drawing upon existing literature, we categorize the simulated distortions into three groups:

- Saliency processing: We add random Gaussian noise to the salient region of I_{ctr} , so that face extraction does not rely on specific facial information but instead only depends on background.
- Global processing: Common global image post-processing operations typically do not introduce noticeable inconsistencies in the background. To simulate such distortions, we apply JPEG compression and global Gaussian noise. Additionally, we observe that, due to the fidelity loss, the watermark’s latent representation is often embedded in high-frequency regions, such as edges

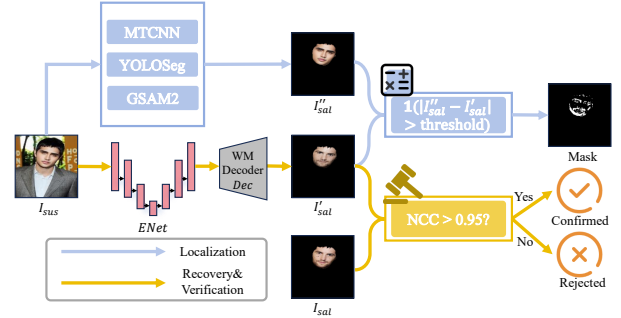


Figure 4. Demonstration of manipulation localization, recovery, and ownership verification for a suspicious image.

of the original image [5, 46]. To account for this, we also incorporate a low-pass filter during distortion.

- Advanced attack: We include a state-of-the-art regeneration attack [54], which can achieve nearly 100% watermark removal success in their experiments. By training to withstand this strongest form of attack, the model is expected to generalize and maintain robustness against other less challenging distortions.

To enhance training stability, instead of applying all distortions from the beginning, we employ a progressive training strategy. Training starts with the most challenging regeneration attack, which occupies half of the total epochs. The remaining distortions are then introduced sequentially, each allocated an equal portion of the remaining half of the training epochs. As we will discuss in Section 5.4, we note that the ordering is crucial in our experiments: introducing the regeneration attack first substantially enhances robustness, whereas delaying it prevents RecoverMark from effectively defending against the strongest attack.

4.3. Recovery, Localization, and Copyright Verification

As illustrated in Figure 4, after recovering the hidden face information I'_{sal} from a suspicious image I_{sus} , RecoverMark proceeds with two distinct stages: manipulation localization and copyright verification. For localization, we iden-

tify tampered regions by comparing I'_{sal} with the saliency of I_{sus} and consequently generate a difference mask. For copyright verification, I'_{sal} is compared with the original face I_{sal} . Ownership is confirmed if the Normalized Correlation Coefficient (NCC), a metric widely used in watermarking literature [2, 46], exceeds 0.95.

5. Experimental Results

5.1. Experimental Settings

5.1.1. Datasets

We conduct our experiments on two public human face datasets. We use CelebA [22] for both training and in-distribution (ID) testing. To evaluate the generalization capability of RecoverMark, we employ FFHQ [14] as an out-of-distribution (OOD) test set. All images are set to 256×256 in RGB format.

5.1.2. Evaluation Metrics

We assess our method’s performance across three tasks. For manipulation localization, we measure the F1 score and the Area Under the Curve (AUC). For facial information recovery, we use the Peak Signal-to-Noise Ratio (PSNR) and the Multiscale Structural Similarity Index (MS-SSIM) [39]. Finally, for ownership verification, we define the Success Rate as the percentage of images where the NCC between I'_{sal} and I_{sal} exceeds the 0.95 threshold.

5.1.3. Implementation Details

For our network architectures, we employ a UNet [31] for *HNet* and use CEILNet [7] for the *Enc*, *Dec*, and *ENet*. Both training stages are optimized using the Adam optimizer with a learning rate of 0.0002. The loss weighting parameters α_1 , α_2 , and α_3 in (11) are all set to 1 and the threshold for binary localization mask generation is set to 0.15. Additionally, all experiments are conducted on a server with an NVIDIA GTX 5880 GPU.

5.2. Qualitative Evaluation

We first present the qualitative evaluation of RecoverMark. As illustrated in Figure 1, before face manipulation, watermark removal attacks such as low-pass filtering and regeneration attack are employed and do not significantly modify the background. While all proactive baselines, including Imuge+ [44], EditGuard [52], and OmniGuard [53], fails to localize the manipulation, our proposed RecoverMark succeeds in precise pixel-level localization. We demonstrate RecoverMark’s robustness to a sequence of cumulative attacks in Figure 5. The attack sequence commences with a regeneration attack, followed by noise, JPEG compression, a low-pass filter, the lattice attack [21], and finally a patch removal attack. It is particularly noteworthy that RecoverMark maintains its robustness even against the lattice



Figure 5. Demonstration of RecoverMark’s robustness against a range of attacks (from single to multiple), including the unseen lattice attack [21], arranged from top to bottom and left to right..

attack, which was not included in the distortion layer during training, highlighting its strong generalization capabilities.

5.3. Quantitative Evaluation

Robustness and Generalizability. As shown in Tables 1 – 4, we benchmark RecoverMark against passive (MVSS-Net [6], HiFiNet [9]) and proactive (Imuge+ [44], EditGuard [52], OmniGuard [53]) methods on ID and OOD datasets. The evaluation covers manipulations from Struct-pix2pix [4] and Stable Diffusion [30] inpaint under a wide range of attacks, including the unseen lattice attack. The results show that RecoverMark maintains exceptional robustness and generalization, significantly outperforming all baselines in localization and recovery metrics across most test conditions.

Capacity Evaluation. We now evaluate the watermark capacity of our proposed method. As illustrated in Figure 6, subfigures (a) and (b) show the fidelity of the recovered saliency I'_{sal} and the watermarked background I_{ctr} , respectively, under the regeneration attack as the saliency-to-image percentage varies. The results show a clear trend that as the facial region percentage increases, the fidelity of both the recovered saliency and the watermarked background gradually decreases. We observe that fidelity remains at a high level when the facial region percentage is 60% or less. Beyond this, the decline becomes more obvious, indicating that a larger payload (i.e., a bigger face) strains the limited capacity of the background, consequently leading to fidelity reduction.

Ownership Verification. As described in Section 4.3, we adopt a NCC threshold of 0.95 for ownership verification. Across all test settings, RecoverMark achieves a Success Rate of 99.9% in ownership verification, demonstrating its effectiveness as a copyright verification mechanism.

Table 1. Quantitative comparison on the ID dataset (CelebA [22]) under Structpix2pix [4] manipulation.

	Method	Localization											
		Regeneration		Patch Remove		Noise		JPEG		LP Filter		Lattice [21]	
		F1	AUC	F1	AUC	F1	AUC	F1	AUC	F1	AUC	F1	AUC
Proactive	MVSS-Net [6]	0.041	0.723	0.025	0.685	0.062	0.711	0.157	0.776	0.184	0.755	0.034	0.719
	HiFiNet [9]	0.048	0.522	0.020	0.531	0.022	0.553	0.080	0.608	0.067	0.552	0.051	0.556
	Imuge+ [44]	0.091	0.587	0.217	0.835	0.016	0.639	0.419	0.956	0.087	0.530	0.010	0.585
	EditGuard [52]	0.090	0.610	0.243	0.888	0.528	0.932	0.552	0.954	0.090	0.658	0.438	0.930
	OmniGuard [53]	0.105	0.655	0.535	0.960	0.127	0.659	0.315	0.890	0.146	0.743	0.113	0.689
	RecoverMark (Ours)	0.855	0.993	0.564	0.974	0.876	0.992	0.867	0.993	0.830	0.989	0.842	0.991
	Method	Recovery											
		Regeneration		Patch Remove		Noise		JPEG		LP Filter		Lattice [21]	
		PSNR	MS-SSIM	PSNR	MS-SSIM	PSNR	MS-SSIM	PSNR	MS-SSIM	PSNR	MS-SSIM	PSNR	MS-SSIM
	Imuge+ [44]	7.252	0.339	14.445	0.673	10.432	0.563	10.778	0.629	10.972	0.603	9.089	0.424
	RecoverMark (Ours)	22.154	0.607	16.624	0.467	23.276	0.657	23.314	0.680	21.744	0.660	23.230	0.655

Table 2. Quantitative comparison on the ID dataset (CelebA [22]) under Stable Diffusion [30] Inpaint manipulation.

	Method	Localization											
		Regeneration		Patch Remove		Noise		JPEG		LP Filter		Lattice [21]	
		F1	AUC	F1	AUC	F1	AUC	F1	AUC	F1	AUC	F1	AUC
Proactive	MVSS-Net [6]	0.257	0.810	0.245	0.786	0.139	0.750	0.213	0.776	0.280	0.726	0.050	0.700
	HiFiNet [9]	0.058	0.635	0.041	0.621	0.002	0.544	0.050	0.607	0.091	0.695	0.031	0.625
	Imuge+ [44]	0.195	0.782	0.442	0.915	0.012	0.655	0.983	0.862	0.186	0.628	0.034	0.546
	EditGuard [52]	0.176	0.580	0.434	0.970	0.792	0.990	0.835	0.995	0.176	0.580	0.704	0.989
	OmniGuard [53]	0.064	0.536	0.911	0.999	0.231	0.693	0.547	0.920	0.273	0.753	0.275	0.757
	RecoverMark (Ours)	0.721	0.992	0.569	0.977	0.759	0.994	0.771	0.994	0.699	0.989	0.756	0.993
	Method	Recovery											
		Regeneration		Patch Remove		Noise		JPEG		LP Filter		Lattice [21]	
		PSNR	MS-SSIM	PSNR	MS-SSIM	PSNR	MS-SSIM	PSNR	MS-SSIM	PSNR	MS-SSIM	PSNR	MS-SSIM
	Imuge+ [44]	11.997	0.318	22.673	0.702	18.296	0.544	21.544	0.671	13.865	0.397	17.643	0.487
	RecoverMark (Ours)	22.553	0.610	17.236	0.491	23.421	0.659	23.745	0.681	21.113	0.621	23.304	0.656

Table 3. Quantitative comparison on the OOD dataset (FFHQ [14]) under Instructpix2pix [4] manipulation.

	Method	Localization											
		Regeneration		Patch Remove		Noise		JPEG		LP Filter		Lattice [21]	
		F1	AUC	F1	AUC	F1	AUC	F1	AUC	F1	AUC	F1	AUC
Proactive	MVSS-Net [6]	0.076	0.686	0.042	0.668	0.049	0.678	0.171	0.776	0.241	0.803	0.028	0.652
	HiFiNet [9]	0.059	0.511	0.003	0.512	0.025	0.526	0.063	0.537	0.024	0.503	0.050	0.561
	Imuge+ [44]	0.081	0.556	0.269	0.867	0.045	0.593	0.463	0.962	0.142	0.763	0.030	0.546
	EditGuard [52]	0.108	0.612	0.286	0.897	0.572	0.940	0.601	0.957	0.115	0.561	0.483	0.932
	OmniGuard [53]	0.124	0.664	0.599	0.975	0.147	0.684	0.333	0.882	0.134	0.660	0.127	0.676
	RecoverMark (Ours)	0.884	0.997	0.585	0.978	0.904	0.998	0.893	0.996	0.853	0.995	0.882	0.997
	Method	Recovery											
		Regeneration		Patch Remove		Noise		JPEG		LP Filter		Lattice [21]	
		PSNR	MS-SSIM	PSNR	MS-SSIM	PSNR	MS-SSIM	PSNR	MS-SSIM	PSNR	MS-SSIM	PSNR	MS-SSIM
	Imuge+ [44]	9.531	0.327	14.075	0.590	14.040	0.541	15.332	0.608	12.081	0.517	13.427	0.421
	RecoverMark (Ours)	22.052	0.593	16.951	0.476	23.215	0.642	23.124	0.657	20.618	0.607	22.993	0.637

5.4. Ablation Study

We conduct two ablation studies to analyze the impact of the distortion layer and the distortion order. On the one hand, as illustrated in Figure 7, RecoverMark trained with only Stage 1 (no distortion layer applied) fails to clearly recover the original face under removal attacks. On the other hand, as demonstrated in Figure 8, we find that the distortion order is crucial and observe that introducing the regeneration attack as the first distortion in the progressive train-

ing pipeline yields superior results. However, if it is placed later in the sequence, RecoverMark fails to develop effective robustness against these attacks. Our conjecture is that employing the most powerful regeneration attack first sets a high standard for robustness early on, guiding the model towards a globally robust embedding rather than allowing it to converge on a “lazy” local minimum effective only against simpler distortions.

Table 4. Quantitative comparison on the OOD dataset (FFHQ [14]) under Stable Diffusion [30] Inpaint manipulation.

Method	Localization												
	Regeneration		Patch Remove		Noise		JPEG		LP Filter		Lattice [21]		
	F1	AUC	F1	AUC	F1	AUC	F1	AUC	F1	AUC	F1	AUC	
Passive	MVSS-Net [6]	0.215	0.805	0.155	0.813	0.071	0.773	0.189	0.789	0.348	0.763	0.012	0.713
	HiFiNet [9]	0.071	0.628	0.041	0.621	0.002	0.605	0.068	0.648	0.128	0.706	0.031	0.659
	Imuge+ [44]	0.219	0.774	0.470	0.924	0.012	0.589	0.672	0.987	0.207	0.661	0.008	0.537
Proactive	EditGuard [52]	0.196	0.583	0.458	0.968	0.800	0.989	0.839	0.996	0.196	0.758	0.711	0.987
	OmniGuard [53]	0.152	0.611	0.895	0.999	0.271	0.735	0.552	0.913	0.254	0.696	0.235	0.7778
	RecoverMark (Ours)	0.732	0.993	0.603	0.976	0.753	0.993	0.759	0.994	0.716	0.987	0.754	0.992

Method	Recovery											
	Regeneration		Patch Remove		Noise		JPEG		LP Filter		Lattice [21]	
	PSNR	MS-SSIM	PSNR	MS-SSIM	PSNR	MS-SSIM	PSNR	MS-SSIM	PSNR	MS-SSIM	PSNR	MS-SSIM
Imuge+ [44]	11.975	0.314	22.51	0.691	17.993	0.531	21.500	0.663	13.964	0.399	17.464	0.474
RecoverMark (Ours)	22.103	0.591	17.225	0.487	23.221	0.641	23.176	0.657	20.623	0.607	23.031	0.638

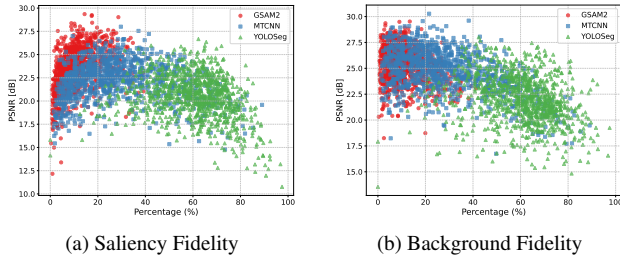


Figure 6. Empirical watermark capacity evaluated by the fidelity of recovered saliency and watermarked background at varying saliency-to-image percentages, measured under regeneration attack.

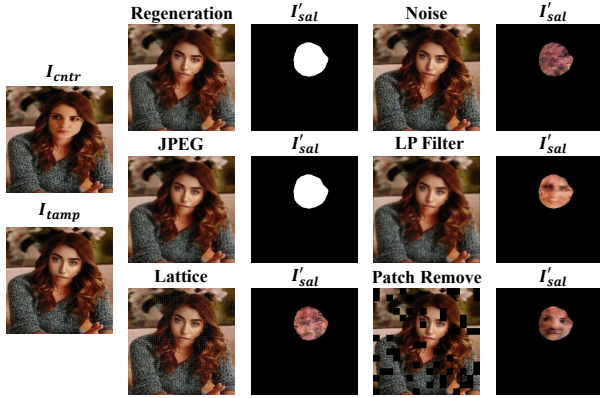


Figure 7. Ablation study on the contribution of the distortion layer to RecoverMark.



Figure 8. Ablation study on the impact of the distortion order.

6. Further Discussion

While RecoverMark demonstrates significant robustness against watermark removal attacks and achieves image manipulation localization, recovery, and ownership verification at the same time, in this paper, we limit the scope only to facial region. However, it is easy to generalize the idea to protect other object categories by segmenting a different salient object as the watermark and using its corresponding background as the container. Regarding limitation, the method is limited by an inherent capacity trade-off. As discussed in Section 5.3, in extreme cases, such as close-up portraits where the facial region is large and the background area is minimal, the limited background capacity may be insufficient to store a high-fidelity watermark, reducing both embedded background and quality of the recovered image. Therefore, higher-capacity robust watermarking techniques also merit further investigation.

7. Conclusion

In this paper, we have introduced RecoverMark, a robust framework that addresses the overlooked vulnerability of existing methods when subjected to watermark removal attacks prior to manipulation. Our method leverages the practical constraint of background consistency, treating the face content itself as a watermark and embedding it into the background to achieve image manipulation localization, recovery, and ownership verification simultaneously. In addition, we have proposed a two-stage, progressive training pipeline that further enhances RecoverMark’s robustness. Extensive experiments show that RecoverMark successfully achieves manipulation localization, recovery, and ownership verification, demonstrating strong generalizability to both seen and unseen attacks, as well as ID and OOD data. We believe that RecoverMark offers significant insights and will inspire future work extending this paradigm to generic images with non-facial saliency.

Acknowledgment

The research work described in this paper was conducted in the JC STEM Lab of Smart City funded by The Hong Kong Jockey Club Charities Trust under Contract 2023-0108. This work was also supported in part by the Hong Kong SAR Government under the Global STEM Professorship and Research Talent Hub, by Singapore Ministry of Education (MOE) under the Academic Research Fund (AcRF) Tier 1 Grant R-MA123-R205-0008, and by the National Research Foundation Singapore under the AI Singapore Programme (AISG Award No: AISG3-RPGV-2025-019). We sincerely appreciate the support provided.

References

- [1] OurMidland News Agency. Whitmer signs bipartisan bills criminalizing sexual ai deepfakes, 2025. News article on Michigan criminalizing non-consensual sexual deepfake creation and distribution. [2](#)
- [2] Haonan An, Guang Hua, Zhengru Fang, Guowen Xu, Susanto Rahardja, and Yuguang Fang. Decoder gradient shield: Provable and high-fidelity prevention of gradient-based box-free watermark removal. In *Proceedings of the Computer Vision and Pattern Recognition Conference*, pages 13424–13433, 2025. [6](#)
- [3] Vishal Asnani, Xi Yin, Tal Hassner, Sijia Liu, and Xiaoming Liu. Proactive image manipulation detection. In *Proceedings of the IEEE/CVF conference on computer vision and pattern recognition*, pages 15386–15395, 2022. [2](#), [3](#)
- [4] Tim Brooks, Aleksander Holynski, and Alexei A Efros. Instructpix2pix: Learning to follow image editing instructions. *arXiv preprint arXiv:2211.09800*, 2022. [6](#), [7](#)
- [5] Huajie Chen, Tianqing Zhu, Chi Liu, Shui Yu, and Wanlei Zhou. High-frequency matters: attack and defense for image-processing model watermarking. *IEEE Transactions on Services Computing*, 17(4):1565–1579, 2024. [5](#)
- [6] Chengbo Dong, Xinru Chen, Ruohan Hu, Juan Cao, and Xirong Li. Mvss-net: Multi-view multi-scale supervised networks for image manipulation detection. *IEEE Transactions on Pattern Analysis and Machine Intelligence*, 45(3):3539–3553, 2022. [2](#), [3](#), [6](#), [7](#), [8](#)
- [7] Qingnan Fan, Jiaolong Yang, Gang Hua, Baoquan Chen, and David Wipf. A generic deep architecture for single image reflection removal and image smoothing. In *IEEE International Conference on Computer Vision (ICCV)*, 2017. [6](#)
- [8] Ian Goodfellow, Jean Pouget-Abadie, Mehdi Mirza, Bing Xu, David Warde-Farley, Sherjil Ozair, Aaron Courville, and Yoshua Bengio. Generative adversarial networks. *Communications of the ACM*, 63(11):139–144, 2020. [1](#)
- [9] Xiao Guo, Xiaohong Liu, Zhiyuan Ren, Steven Grosz, Iacopo Masi, and Xiaoming Liu. Hierarchical fine-grained image forgery detection and localization. In *Proceedings of the IEEE/CVF conference on computer vision and pattern recognition*, pages 3155–3165, 2023. [3](#), [6](#), [7](#), [8](#)
- [10] HongJie He, JiaShu Zhang, and Heng-Ming Tai. A wavelet-based fragile watermarking scheme for secure image authentication. In *International workshop on digital watermarking*, pages 422–432. Springer, 2006. [3](#)
- [11] Senkang Hu, Yihang Tao, Guowen Xu, Yiqin Deng, Xianhao Chen, Yuguang Fang, and Sam Kwong. Cp-guard: malicious agent detection and defense in collaborative bird’s eye view perception. In *Proceedings of the Thirty-Ninth AAAI Conference on Artificial Intelligence and Thirty-Seventh Conference on Innovative Applications of Artificial Intelligence and Fifteenth Symposium on Educational Advances in Artificial Intelligence*. AAAI Press, 2025. [2](#)
- [12] Xiaoxiao Hu, Qichao Ying, Zhenxing Qian, Sheng Li, and Xinpeng Zhang. Draw: Defending camera-shooted raw against image manipulation. In *Proceedings of the IEEE/CVF International Conference on Computer Vision*, pages 22434–22444, 2023. [2](#)
- [13] Ashraf Islam, Chengjiang Long, Arslan Basharat, and Anthony Hoogs. Doa-gan: Dual-order attentive generative adversarial network for image copy-move forgery detection and localization. In *Proceedings of the IEEE/CVF conference on computer vision and pattern recognition*, pages 4676–4685, 2020. [3](#)
- [14] Tero Karras, Samuli Laine, and Timo Aila. A style-based generator architecture for generative adversarial networks. In *Proceedings of the IEEE/CVF conference on computer vision and pattern recognition*, pages 4401–4410, 2019. [6](#), [7](#), [8](#)
- [15] Tero Karras, Samuli Laine, and Timo Aila. A style-based generator architecture for generative adversarial networks. In *Proceedings of the IEEE/CVF conference on computer vision and pattern recognition*, pages 4401–4410, 2019. [1](#)
- [16] Eric Kee, James F O’Brien, and Hany Farid. Exposing photo manipulation with inconsistent shadows. *ACM Transactions on Graphics (ToG)*, 32(3):1–12, 2013. [2](#)
- [17] Chenqi Kong, Baoliang Chen, Haoliang Li, Shiqi Wang, Anderson Rocha, and Sam Kwong. Detect and locate: Exposing face manipulation by semantic-and noise-level telltales. *IEEE Transactions on Information Forensics and Security*, 17:1741–1756, 2022. [2](#)
- [18] Haodong Li and Jiwu Huang. Localization of deep inpainting using high-pass fully convolutional network. In *Proceedings of the IEEE/CVF international conference on computer vision*, pages 8301–8310, 2019. [3](#)
- [19] Tao Li, Yulin Tang, Yiyang Song, Cong Wu, Xihui Liu, Pan Li, and Xianhao Chen. Splitcom: Communication-efficient split federated fine-tuning of llms via temporal compression. *arXiv preprint arXiv:2602.10564*, 2026. [2](#)
- [20] Zhouchen Lin, Junfeng He, Xiaoou Tang, and Chi-Keung Tang. Fast, automatic and fine-grained tampered jpeg image detection via dct coefficient analysis. *Pattern Recognition*, 42(11):2492–2501, 2009. [2](#)
- [21] Hangcheng Liu, Tao Xiang, Shangwei Guo, Han Li, Tianwei Zhang, and Xiaofeng Liao. Erase and repair: An efficient box-free removal attack on high-capacity deep hiding. *IEEE Transactions on Information Forensics and Security*, 18:5229–5242, 2023. [2](#), [6](#), [7](#), [8](#)
- [22] Ziwei Liu, Ping Luo, Xiaogang Wang, and Xiaoou Tang. Deep learning face attributes in the wild. In *Proceedings of*

- International Conference on Computer Vision (ICCV)*, 2015. 6, 7
- [23] Zijie Lou, Gang Cao, Kun Guo, Lifang Yu, and Shaowei Weng. Exploring multi-view pixel contrast for general and robust image forgery localization. *IEEE Transactions on Information Forensics and Security*, 2025. 3
- [24] Siwei Lyu, Xunyu Pan, and Xing Zhang. Exposing region splicing forgeries with blind local noise estimation. *International journal of computer vision*, 110(2):202–221, 2014. 2
- [25] Fahim Faisal Niloy, Kishor Kumar Bhaumik, and Simon S Woo. Cfl-net: Image forgery localization using contrastive learning. In *Proceedings of the IEEE/CVF winter conference on applications of computer vision*, pages 4642–4651, 2023. 3
- [26] Aberna Palani and Agilandeewari Loganathan. Semi-blind watermarking using convolutional attention-based turtle shell matrix for tamper detection and recovery of medical images. *Expert Systems with Applications*, 238:121903, 2024. 3
- [27] PetaPixel. Scarlett johansson takes legal action against ai app that used her image, 2023. Scarlett Johansson sues AI app for unauthorized use of her likeness. 2
- [28] Nikhila Ravi, Valentin Gabeur, Yuan-Ting Hu, Ronghang Hu, Chaitanya Ryali, Tengyu Ma, Haitham Khedr, Roman Rädle, Chloe Rolland, Laura Gustafson, et al. Sam 2: Segment anything in images and videos. *arXiv preprint arXiv:2408.00714*, 2024. 4
- [29] Tianhe Ren, Shilong Liu, Ailing Zeng, Jing Lin, Kunchang Li, He Cao, Jiayu Chen, Xinyu Huang, Yukang Chen, Feng Yan, et al. Grounded sam: Assembling open-world models for diverse visual tasks. *arXiv preprint arXiv:2401.14159*, 2024. 1
- [30] Robin Rombach, Andreas Blattmann, Dominik Lorenz, Patrick Esser, and Björn Ommer. High-resolution image synthesis with latent diffusion models. In *Proceedings of the IEEE/CVF conference on computer vision and pattern recognition*, pages 10684–10695, 2022. 1, 6, 7, 8
- [31] Olaf Ronneberger, Philipp Fischer, and Thomas Brox. U-net: Convolutional networks for biomedical image segmentation. In *International Conference on Medical image computing and computer-assisted intervention*, pages 234–241. Springer, 2015. 6
- [32] Nataniel Ruiz, Sarah Adel Bargal, and Stan Sclaroff. Disrupting deepfakes: Adversarial attacks against conditional image translation networks and facial manipulation systems. In *European conference on computer vision*, pages 236–251. Springer, 2020. 3
- [33] Ronald Salloum, Yuzhuo Ren, and C-C Jay Kuo. Image splicing localization using a multi-task fully convolutional network (mfcn). *Journal of Visual Communication and Image Representation*, 51:201–209, 2018. 2
- [34] South China Morning Post. “Everyone looked real”: multinational firm’s Hong Kong office loses HK\$200 million after scammers stage deepfake video meeting, 2024. News article; deepfake video conference financial scam. 2
- [35] Yihang Tao, Senkang Hu, Zhengru Fang, and Yuguang Fang. Directed-cp: Directed collaborative perception for connected and autonomous vehicles via proactive attention. In *2025 IEEE International Conference on Robotics and Automation (ICRA)*, pages 7004–7010, 2025. 2
- [36] Yihang Tao, Senkang Hu, Yue Hu, Haonan An, Hangcheng Cao, and Yuguang Fang. Gcp: Guarded collaborative perception with spatial-temporal aware malicious agent detection, 2025. 2
- [37] Ultralytics. Ultralytics yolo. <https://github.com/ultralytics/ultralytics>, 2025. 1, 4
- [38] Run Wang, Felix Juefei-Xu, Meng Luo, Yang Liu, and Lina Wang. Faketagger: Robust safeguards against deepfake dissemination via provenance tracking. In *Proceedings of the 29th ACM international conference on multimedia*, pages 3546–3555, 2021. 3
- [39] Zhou Wang, Eero P Simoncelli, and Alan C Bovik. Multi-scale structural similarity for image quality assessment. In *The thirty-seventh asilomar conference on signals, systems & computers, 2003*, pages 1398–1402. Ieee, 2003. 6
- [40] Yue Wu, Wael AbdAlmageed, and Premkumar Natarajan. Mantra-net: Manipulation tracing network for detection and localization of image forgeries with anomalous features. In *Proceedings of the IEEE/CVF conference on computer vision and pattern recognition*, pages 9543–9552, 2019. 2, 3
- [41] Chin-Yuan Yeh, Hsi-Wen Chen, Shang-Lun Tsai, and Sheng-De Wang. Disrupting image-translation-based deepfake algorithms with adversarial attacks. In *Proceedings of the IEEE/CVF Winter Conference on Applications of Computer Vision Workshops*, pages 53–62, 2020. 3
- [42] Qichao Ying, Zhenxing Qian, Hang Zhou, Haisheng Xu, Xinpeng Zhang, and Siyi Li. From image to imuge: Immunized image generation. In *Proceedings of the 29th ACM international conference on Multimedia*, pages 3565–3573, 2021. 2, 3
- [43] Qichao Ying, Xiaoxiao Hu, Xiangyu Zhang, Zhenxing Qian, Sheng Li, and Xinpeng Zhang. Rwn: Robust watermarking network for image cropping localization. In *2022 IEEE International Conference on Image Processing (ICIP)*, pages 301–305. IEEE, 2022. 3
- [44] Qichao Ying, Hang Zhou, Zhenxing Qian, Sheng Li, and Xinpeng Zhang. Learning to immunize images for tamper localization and self-recovery. *IEEE Transactions on Pattern Analysis and Machine Intelligence*, 45(11):13814–13830, 2023. 1, 2, 3, 6, 7, 8
- [45] Zeqin Yu, Jiangqun Ni, Yuzhen Lin, Haoyi Deng, and Bin Li. Difforensics: Leveraging diffusion prior to image forgery detection and localization. In *Proceedings of the IEEE/CVF Conference on Computer Vision and Pattern Recognition*, pages 12765–12774, 2024. 3
- [46] Jie Zhang, Dongdong Chen, Jing Liao, Zehua Ma, Han Fang, Weiming Zhang, Huamin Feng, Gang Hua, and Nenghai Yu. Robust model watermarking for image processing networks via structure consistency. *IEEE Transactions on Pattern Analysis and Machine Intelligence*, 46(10):6985–6992, 2024. 5, 6
- [47] Kaipeng Zhang, Zhanpeng Zhang, Zhifeng Li, and Yu Qiao. Joint face detection and alignment using multitask cascaded convolutional networks. *IEEE signal processing letters*, 23(10):1499–1503, 2016. 1, 4, 5

- [48] Xinpeng Zhang and Shuozhong Wang. Fragile watermarking with error-free restoration capability. *IEEE Transactions on Multimedia*, 10(8):1490–1499, 2008. [3](#)
- [49] Xinpeng Zhang and Shuozhong Wang. Fragile watermarking scheme using a hierarchical mechanism. *Signal processing*, 89(4):675–679, 2009. [3](#)
- [50] Xinpeng Zhang, Shuozhong Wang, Zhenxing Qian, and Guorui Feng. Reference sharing mechanism for watermark self-embedding. *IEEE Transactions on Image Processing*, 20(2):485–495, 2010.
- [51] Xinpeng Zhang, Zhenxing Qian, Yanli Ren, and Guorui Feng. Watermarking with flexible self-recovery quality based on compressive sensing and compositive reconstruction. *IEEE Transactions on Information Forensics and Security*, 6(4):1223–1232, 2011. [3](#)
- [52] Xuanyu Zhang, Runyi Li, Jiwen Yu, Youmin Xu, Weiqi Li, and Jian Zhang. Editguard: Versatile image watermarking for tamper localization and copyright protection. In *Proceedings of the IEEE/CVF conference on computer vision and pattern recognition*, pages 11964–11974, 2024. [1](#), [2](#), [3](#), [6](#), [7](#), [8](#)
- [53] Xuanyu Zhang, Zecheng Tang, Zhipei Xu, Runyi Li, Youmin Xu, Bin Chen, Feng Gao, and Jian Zhang. Omniguard: Hybrid manipulation localization via augmented versatile deep image watermarking. In *Proceedings of the Computer Vision and Pattern Recognition Conference*, pages 3008–3018, 2025. [1](#), [2](#), [3](#), [6](#), [7](#), [8](#)
- [54] Xuandong Zhao, Kexun Zhang, Zihao Su, Saastha Vasani, Ilya Grishchenko, Christopher Kruegel, Giovanni Vigna, Yu-Xiang Wang, and Lei Li. Invisible image watermarks are provably removable using generative ai. *Advances in neural information processing systems*, 37:8643–8672, 2024. [1](#), [2](#), [5](#)
- [55] Yuan Zhao, Bo Liu, Tianqing Zhu, Ming Ding, Xin Yu, and Wanlei Zhou. Proactive image manipulation detection via deep semi-fragile watermark. *Neurocomputing*, 585:127593, 2024. [3](#)
- [56] Peng Zhou, Xintong Han, Vlad I Morariu, and Larry S Davis. Learning rich features for image manipulation detection. In *Proceedings of the IEEE conference on computer vision and pattern recognition*, pages 1053–1061, 2018. [3](#)